

# Interacting model of new agegraphic dark energy: observational constraints and age problem

Yun-He Li,<sup>1</sup> Jing-Zhe Ma,<sup>1</sup> Jing-Lei Cui,<sup>1</sup> Zhuo Wang,<sup>1</sup> and Xin Zhang<sup>\*1,2,†</sup>

<sup>1</sup>*Department of Physics, College of Sciences, Northeastern University, Shenyang 110004, China*

<sup>2</sup>*Center for High Energy Physics, Peking University, Beijing 100080, China*

Many dark energy models fail to pass the cosmic age test because of the old quasar APM 08279+5255 at redshift  $z = 3.91$ , the  $\Lambda$ CDM model and holographic dark energy models being no exception. In this paper, we focus on the topic of age problem in the new agegraphic dark energy (NADE) model. We determine the age of the universe in the NADE model by fitting the observational data, including type Ia supernovae (SNIa), baryon acoustic oscillations (BAO) and the cosmic microwave background (CMB). We find that the NADE model also faces the challenge of the age problem caused by the old quasar APM 08279+5255. In order to overcome such a difficulty, we consider the possible interaction between dark energy and dark matter. We show that this quasar can be successfully accommodated in the interacting new agegraphic dark energy (INADE) model at the  $2\sigma$  level under the current observational constraints.

PACS numbers: 95.36.+x, 98.80.Es, 98.80.-k

## I. INTRODUCTION

At its present stage, our universe is undergoing an accelerated expansion, which has been confirmed by many astronomical observations, such as, type Ia supernovae (SNIa) [1], large scale structure (LSS) [2] and the cosmic microwave background (CMB) [3], among others. All these observations indicate the existence of a “dark energy” with negative pressure. The most important theoretical candidate for dark energy is the cosmological constant,  $\Lambda$ , which fits the observations well, but is plagued with some severe theoretical difficulties, such as the so called “fine-tuning” and “cosmic coincidence” problems [4]. During the past decade, in order to unveil its nature, theorists have proposed many phenomenological models of dark energy, e.g., quintessence [5],  $k$ -essence [6], tachyon [7], phantom [8], quintom [9], braneworld [10], and Chaplygin gas [11]. Further, the possibility that dark energy might interact with dark matter, owing to their unknown nature, has also been seriously considered in many works to help solve the cosmic coincidence problem [12] and the cosmic doomsday problem [13]. For reviews of dark energy, see, e.g., [14].

In recent years, it has been found that many dark energy models get into trouble when tested by some old high redshift objects (OHROs). It is obvious that the universe cannot be younger than its constituents, so the age of some astronomical objects (at some redshift), if measured accurately, can be used to test cosmological models according to this simple age principle. There have been some OHROs discovered, including, the 3.5 Gyr old galaxy LBDS 53W091 at redshift  $z = 1.55$  [15] and the 4.0 Gyr old galaxy LBDS 53W069 at redshift  $z = 1.43$  [16]. In particular, the old quasar

APM 08279 + 5255 at redshift  $z = 3.91$  is an important one, which has been used as a “cosmic clock” to constrain cosmological models. Its age is estimated to be 2.0 – 3.0 Gyr [17]. These three OHROs at  $z = 1.43, 1.55$  and 3.91 have been used to test many dark energy models, including, the  $\Lambda$ CDM model [18], the general EoS dark energy model [19], the scalar-tensor quintessence model [20], the  $f(R) = \sqrt{R^2 - R_0^2}$  model [21], the DGP braneworld model [22], the power-law parameterized quintessence model [23], the Yang-Mills condensate model [24], the holographic dark energy model [25], and the agegraphic dark energy model [26]. These investigations show that the two OHROs at  $z = 1.43$  and 1.55 can be easily accommodated in most dark energy models, whereas the OHRO at  $z = 3.91$  cannot, even in the  $\Lambda$ CDM model [18] and the holographic dark energy model [25]. In this paper, we will investigate the cosmic age problem in the new agegraphic dark energy (NADE) model. We will show that the NADE model also faces the challenge of such an age problem. In order to escape from the cosmic age crisis, we consider the possible interaction between dark energy and dark matter. We will check whether the age problem can be solved successfully in the interacting new agegraphic dark energy (INADE) model. Of course, our discussions are based on the current observational constraints on the models. So, we will first place observational constraints on the NADE and INADE models, and then discuss the cosmic age problem.

## II. THE NEW AGEGRAPHIC DARK ENERGY MODEL WITH INTERACTION

In this section, we describe the INADE model in a flat universe. Many theorists believe that we cannot entirely understand the nature of dark energy before a complete theory of quantum gravity is established [27]. In the circumstance that a full theory of quantum gravity is not yet available, it is more realistic to consider the possible cos-

\*Corresponding author

†Electronic address: zhangxin@mail.neu.edu.cn

mological consequences of some fundamental principles of quantum gravity. The holographic principle [28] is commonly believed to be such a principle, so it is expected to play an essential role in investigating dark energy [29]. Along this line, a model of holographic dark energy has been proposed [30] (see also, e.g., [31] and [32]). The agegraphic dark energy model [33] is constructed in light of the Károlyházy relation [34] and corresponding energy fluctuations of space-time. Actually, it has been proven that the agegraphic dark energy scenario is also a kind of holographic model of dark energy [33]. In such a holographic model, the UV problem of dark energy is converted into an IR problem, since the dark energy density is inversely proportional to the square of the IR length scale,  $\rho_{de} \sim L^{-2}$ . In the old version of the agegraphic dark energy model [33], the IR cutoff is chosen as the age of the universe,  $t$  (here it should be pointed out that the speed of light has already been taken to be 1, so time and length have the same dimension). However, there are some inner inconsistencies in this model; for details see [35]. Therefore, in this paper, we only discuss the new version of the agegraphic dark energy model [35].

In the NADE model, the IR cutoff is chosen to be the conformal age of the universe,

$$\eta \equiv \int_0^t \frac{d\tilde{t}}{a} = \int_0^a \frac{d\tilde{a}}{H\tilde{a}^2}, \quad (1)$$

so the energy density of NADE is

$$\rho_q = \frac{3n^2 m_p^2}{\eta^2}, \quad (2)$$

where  $n$  is a numerical parameter and  $m_p$  is the reduced Planck mass.

If we consider a spatially flat FRW universe containing agegraphic dark energy and dark matter, the corresponding Friedmann equation is

$$H^2 = \frac{1}{3m_p^2} (\rho_m + \rho_q), \quad (3)$$

or equivalently,

$$E(z) \equiv \frac{H(z)}{H_0} = \left( \frac{\Omega_{m0}(1+z)^3}{1 - \Omega_q(z)} \right)^{1/2}, \quad (4)$$

where  $\Omega_{m0}$  is the present fractional dark matter density and  $\Omega_q \equiv \rho_q/(3m_p^2 H^2)$ . Note that, for simplicity, in this paper we neglect the contributions from baryons and radiation. From (2), it is easy to find that

$$\Omega_q = \frac{n^2}{H^2 \eta^2}. \quad (5)$$

Obviously,  $\Omega_m \equiv \rho_m/(3m_p^2 H^2) = 1 - \Omega_q$  from (3). By using (1), (2), (3) and (5) and the energy conservation equation  $\dot{\rho}_m + 3H\rho_m = 0$ , we obtain the equation of motion for  $\Omega_q$ :

$$\Omega'_q = \Omega_q (1 - \Omega_q) \left( 3 - \frac{2}{na} \sqrt{\Omega_q} \right), \quad (6)$$

where the prime denotes the derivative with respect to  $x \equiv \ln a$ . Since  $\frac{d}{dx} = -(1+z) \frac{d}{dz}$ , we get

$$\frac{d\Omega_q}{dz} = -\frac{\Omega_q}{1+z} (1 - \Omega_q) \left( 3 - \frac{2(1+z)}{n} \sqrt{\Omega_q} \right). \quad (7)$$

From the energy conservation equation  $\dot{\rho}_q + 3H(\rho_q + p_q) = 0$ , as well as (2) and (5), it is easy to find that the equation-of-state (EoS) parameter of the NADE model is given by

$$w_q = -1 + \frac{2}{3na} \sqrt{\Omega_q}. \quad (8)$$

The NADE model has been studied extensively; see, e.g., [36, 37]. In the following, we shall extend the NADE model by considering the interaction between dark energy and dark matter.

Assuming that dark energy and dark matter exchange energy through the interaction term  $Q$ , the continuity equations become

$$\dot{\rho}_q + 3H(\rho_q + p_q) = -Q \quad (9)$$

and

$$\dot{\rho}_m + 3H\rho_m = Q. \quad (10)$$

Owing to the lack of any knowledge of the micro-origin of the interaction, we simply follow other work on interacting dark energy and parameterize the interaction term generally as  $Q = 3H(\alpha\rho_q + \beta\rho_m)$ , where  $\alpha$  and  $\beta$  are dimensionless coupling constants. In order to reduce both complexity and the number of parameters, one often considers the following three cases: (i)  $\alpha = b$  and  $\beta = 0$ , denoted as INADE1, (ii)  $\alpha = 0$  and  $\beta = b$ , denoted as INADE2, and (iii)  $\alpha = \beta = b$ , denoted as INADE3. Note that according to our convention  $b > 0$  means that dark energy decays to dark matter, while  $b < 0$  means that dark matter decays into dark energy. In cases (i) and (iii), a negative value of  $b$  would lead to the unphysical consequence that  $\rho_m$  becomes negative in the distant future. For negative  $b$  values in case (ii), no such difficulty exists. In [38] it is argued from the thermodynamical view that the second law of thermodynamics strongly favors that dark energy decays into dark matter. So, in general,  $b$  is taken to be positive.

However, recently, it has been found that observations may favor the case of dark matter decaying into dark energy [39, 40]. In particular, in [41], in a way independent of specific interacting forms, the authors fitted for the interaction term  $Q$  using observations. They found that  $Q$  is likely to cross the non-interacting line ( $Q = 0$ ), i.e., the sign of the interaction  $Q$  is changed, around  $z = 0.5$ . This raises a remarkable challenge to the interacting models, since the general phenomenological forms of interaction, as shown in the above, do not provide the possibility of changing signs. As noted in [41], more general forms of interaction should be considered. For this reason, a new form of interaction, (iv)  $\alpha = -\beta = b$ , denoted as INADE4, was considered in [42]. Obviously, for this case,

in the early stage, since  $\rho_m > \rho_q$ ,  $Q$  is negative. However,  $Q$  may change from negative to positive when the expansion of the universe changes from decelerating to accelerating. The parameter  $b$  in this case is also assumed to be positive, since negative  $b$  would lead to a negative  $\rho_m$  in the distant future.

For clarity, we denote the aforementioned interaction term  $Q$  as

$$Q = \begin{cases} 3bH\rho_q, \\ 3bH\rho_m, \\ 3bH(\rho_q + \rho_m), \\ 3bH(\rho_q - \rho_m). \end{cases} \quad (11)$$

Note that in cases (i), (iii) and (iv) the parameter  $b$  is always assumed to be positive in the literature. However, in the present work, instead of making such an assumption, we permit this variable to be completely free and allow the observational data to tell us the true story, no matter if the ultimate fate of the universe is ridiculous or not.

Differentiating (5) with respect to  $\ln a$  and using (1), we get

$$\Omega'_q = \Omega_q \left( -2\frac{\dot{H}}{H^2} - \frac{2}{na} \sqrt{\Omega_q} \right). \quad (12)$$

Differentiating (3) with respect to time  $t$  and combining (1), (5), (9) and (10), we can easily find that

$$-\frac{\dot{H}}{H^2} = \frac{3}{2}(1 - \Omega_q) + \frac{\Omega_q^{3/2}}{na} - \frac{Q}{6m^2H^3}. \quad (13)$$

Therefore, we obtain the equation of motion for  $\Omega_q$ ,

$$\Omega'_q = \Omega_q \left[ (1 - \Omega_q) \left( 3 - \frac{2}{na} \sqrt{\Omega_q} \right) - Q_1 \right], \quad (14)$$

or equivalently,

$$\frac{d\Omega_q}{dz} = -\frac{\Omega_q}{1+z} \left[ (1 - \Omega_q) \left( 3 - \frac{2(1+z)}{n} \sqrt{\Omega_q} \right) - Q_1 \right], \quad (15)$$

where

$$Q_1 \equiv \frac{Q}{3m^2H^3}. \quad (16)$$

From (5) and (9), we get the EoS parameter of dark energy:

$$w_q = -1 + \frac{2}{3na} \sqrt{\Omega_q} - Q_2, \quad (17)$$

where

$$Q_2 \equiv \frac{Q}{3H\rho_q}. \quad (18)$$

It is convenient to define the effective EoS parameters for dark energy and dark matter as

$$w_q^{(e)} = w_q + \frac{Q}{3H\rho_q} \quad (19)$$

and

$$w_m^{(e)} = -\frac{Q}{3H\rho_m}. \quad (20)$$

According to the definition of the effective EoS parameters, the continuity equations for dark energy and dark matter can be re-expressed in the form of energy conservation:

$$\dot{\rho}_q + 3H(1 + w_q^{(e)})\rho_q = 0 \quad (21)$$

and

$$\dot{\rho}_m + 3H(1 + w_m^{(e)})\rho_m = 0. \quad (22)$$

Taking the aforementioned four cases of interaction, one can obtain

$$w_m^{(e)} = \begin{cases} -b\frac{\Omega_q}{1-\Omega_q} & Q = 3bH\rho_q, \\ -b & Q = 3bH\rho_m, \\ -b\left(1 + \frac{\Omega_q}{1-\Omega_q}\right) & Q = 3bH(\rho_q + \rho_m), \\ -b\left(-1 + \frac{\Omega_q}{1-\Omega_q}\right) & Q = 3bH(\rho_q - \rho_m). \end{cases} \quad (23)$$

Now, the Friedmann equation can be expressed as

$$H(z) = H_0 E(z), \quad (24)$$

where

$$E(z) = \left[ \frac{(1 - \Omega_{q0}) e^{3 \int_0^z \frac{1+w_m^{(e)}}{1+z} dz}}{1 - \Omega_q(z)} \right]^{1/2}. \quad (25)$$

In the above equation,  $\Omega_q(z)$  can be obtained by numerically solving (15) with the initial condition  $\Omega_q(z_{ini}) = n^2(1 + z_{ini})^{-2}/4$  at  $z_{ini} = 2000$  [36]. While this initial condition is obtained from a NADE model without interaction in the matter-dominated epoch, it is still suitable to an interacting model of NADE because the contribution of dark energy to the cosmological evolution is negligible in the matter-dominated epoch and therefore its impact can be ignored during that time; for details see [43].

### III. OBSERVATIONAL CONSTRAINTS

In this section, we place observational constraints on the NADE and INADE models. For the data, we will use the combination of SNIa, CMB and BAO.

First, we consider the 557 Union2 SNIa compiled in [44]. The theoretical distance modulus is defined as

$$\mu_{th}(z_i) \equiv 5 \log_{10} D_L(z_i) + \mu_0, \quad (26)$$

where  $\mu_0 \equiv 42.38 - 5 \log_{10} h$  with  $h$  the Hubble constant  $H_0$  in units of  $100 \text{ km s}^{-1} \text{ Mpc}^{-1}$ , and the Hubble-free luminosity distance

$$D_L(z) = (1+z) \int_0^z \frac{d\tilde{z}}{E(\tilde{z}; \mathbf{p})}, \quad (27)$$

where  $E \equiv H/H_0$ , and  $\mathbf{p}$  denotes the model parameters. Correspondingly, the  $\chi^2$  function for the 557 Union2 SNIa data is given by

$$\chi_\mu^2(\mathbf{p}) = \sum_{i=1}^{557} \frac{[\mu_{obs}(z_i) - \mu_{th}(z_i)]^2}{\sigma^2(z_i)}, \quad (28)$$

where  $\sigma$  is the  $1\sigma$  error in distance modulus for each supernova. The parameter  $\mu_0$  is a nuisance parameter but it is independent of the data points. Following [45], the minimization with respect to  $\mu_0$  is easily performed by expanding  $\chi^2$  of (28) with respect to  $\mu_0$  as

$$\chi_\mu^2(\mathbf{p}) = A - 2\mu_0 B + \mu_0^2 C, \quad (29)$$

where

$$A(\mathbf{p}) = \sum_{i=1}^{557} \frac{[\mu_{obs}(z_i) - \mu_{th}(z_i; \mu_0 = 0, \mathbf{p})]^2}{\sigma_{\mu_{obs}}^2(z_i)},$$

$$B(\mathbf{p}) = \sum_{i=1}^{557} \frac{\mu_{obs}(z_i) - \mu_{th}(z_i; \mu_0 = 0, \mathbf{p})}{\sigma_{\mu_{obs}}^2(z_i)},$$

and

$$C = \sum_{i=1}^{557} \frac{1}{\sigma_{\mu_{obs}}^2(z_i)}.$$

It is evident that (29) has a minimum for  $\mu_0 = B/C$  at

$$\tilde{\chi}_\mu^2(\mathbf{p}) = A(\mathbf{p}) - \frac{B(\mathbf{p})^2}{C}. \quad (30)$$

Since  $\chi_{\mu, min}^2 = \tilde{\chi}_{\mu, min}^2$ , instead of minimizing  $\chi_\mu^2$  we will minimize  $\tilde{\chi}_\mu^2$  which is independent of the nuisance parameter  $\mu_0$ . Obviously, the best-fit value of  $h$  can be given by the corresponding  $\mu_0 = B/C$  of the best fit.

Next, we consider the cosmological observational data from WMAP and SDSS. For the WMAP data, we use the CMB shift parameter  $R$ ; for the SDSS data, we use the parameter  $A$  of the BAO measurement. It is widely believed that both  $R$  and  $A$  are nearly model-independent and contain essential information of the full WMAP CMB and SDSS BAO data [46].

The shift parameter  $R$  is given by [46, 47]

$$R \equiv \Omega_{m0}^{1/2} \int_0^{z_*} \frac{d\tilde{z}}{E(\tilde{z})}, \quad (31)$$

where the redshift of recombination  $z_* = 1091.3$  which has been updated in the WMAP 7-year data [48]. The

shift parameter  $R$  relates the angular diameter distance to the last scattering surface, the comoving size of the sound horizon at  $z_*$  and the angular scale of the first acoustic peak in the CMB power spectrum of temperature fluctuations [46, 47]. The value of  $R$  has been updated to  $1.725 \pm 0.018$  from the WMAP 7-year data [48]. On the other hand, the distance parameter  $A$  from the measurement of the BAO peak in the distribution of SDSS luminous red galaxies [49] is given by

$$A \equiv \Omega_{m0}^{1/2} E(z_b)^{-1/3} \left[ \frac{1}{z_b} \int_0^{z_b} \frac{d\tilde{z}}{E(\tilde{z})} \right]^{2/3}, \quad (32)$$

where  $z_b = 0.35$ . In [50], the value of  $A$  has been determined to be  $0.469 (n_s/0.98)^{-0.35} \pm 0.017$ . Here, the scalar spectral index  $n_s$  is taken to be 0.963, which has been updated from the WMAP 7-year data [48]. So the total  $\chi^2$  is given by

$$\chi^2 = \tilde{\chi}_\mu^2 + \chi_{CMB}^2 + \chi_{BAO}^2, \quad (33)$$

where  $\tilde{\chi}_\mu^2$  is given in (30),  $\chi_{CMB}^2 = (R - R_{obs})^2/\sigma_R^2$  and  $\chi_{BAO}^2 = (A - A_{obs})^2/\sigma_A^2$ . The best fit model parameters are determined by minimizing the total  $\chi^2$ . The 68.3% confidence level is determined by  $\Delta\chi^2 \equiv \chi^2 - \chi_{min}^2 \leq 1.0, 2.3$  and  $3.53$  for  $n_p = 1, 2$  and  $3$ , respectively, where  $n_p$  is the number of free model parameters. Similarly, the 95.4% confidence level is determined by  $\Delta\chi^2 \equiv \chi^2 - \chi_{min}^2 \leq 4.0, 6.17$  and  $8.02$  for  $n_p = 1, 2$  and  $3$ , respectively.

Now, let us discuss the observational constraints on the NADE model. The NADE model is a single-parameter model whose sole parameter is  $n$ . Solving (7) numerically with the initial condition  $\Omega_q(z_{ini}) = n^2(1+z_{ini})^{-2}/4$  at  $z_{ini} = 2000$  and substituting the resultant  $\Omega_q(z)$  into (4), the corresponding  $E(z)$  can be obtained.

For the NADE model, the cosmological constraints are found to be:  $n = 2.886_{-0.082}^{+0.084}$  at the  $1\sigma$  level and  $n = 2.886_{-0.163}^{+0.169}$  at the  $2\sigma$  level. The best fit gives values of  $\chi_{min}^2 = 571.338$ ,  $h = 0.685$  and  $\Omega_{m0} = 0.265$ . In Figure 1, we plot the relation of  $\chi^2 - n$  for the NADE model.

According to [35], the NADE model is always considered as a single-parameter model, and the initial condition is chosen to be  $\Omega_q(z_{ini}) = n^2(1+z_{ini})^{-2}/4$  at  $z_{ini} = 2000$ . We can, however, adopt the different perspective of the NADE model being a two-parameter model. In doing so, we are interested in the result the observational data will tell us. To see this, we choose the initial condition  $\Omega_{q0} = 1 - \Omega_{m0}$  for the NADE model, and then it becomes a two-parameter model with the free parameters  $\Omega_{m0}$  and  $n$ . In Figure 2 (Left), we plot contours of the 68.3% and 95.4% confidence levels in the  $\Omega_{m0} - n$  plane for the NADE model. The fit values for the model parameters are also shown in Table I.

Now, with the NADE model being viewed as a two-parameter model, it is of great interest to make a direct comparison with the holographic dark energy (HDE)

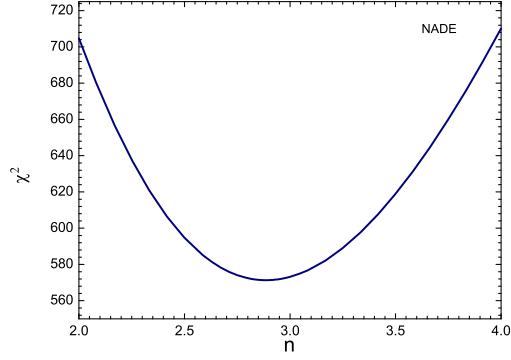


FIG. 1: (color online) The plot of  $\chi^2$  versus  $n$  for the NADE model.

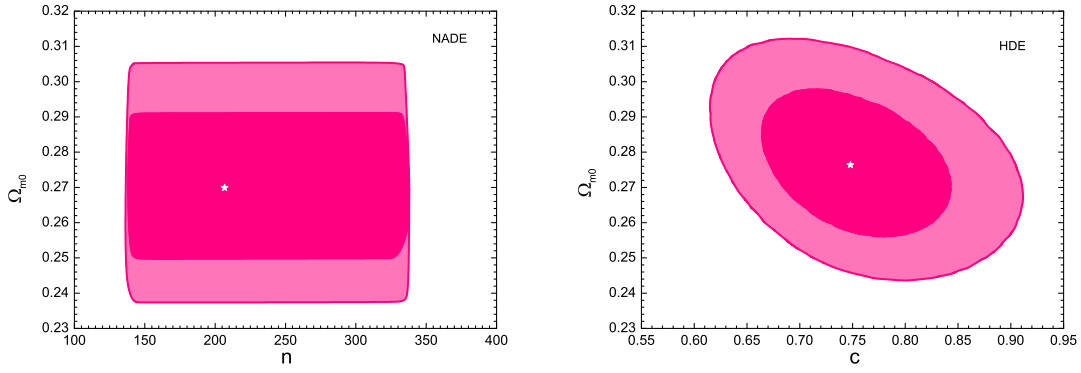


FIG. 2: (color online) The probability contours at  $1\sigma$  and  $2\sigma$  confidence levels in the  $\Omega_{m0} - n$  plane for the NADE model (*Left*) and in the  $\Omega_{m0} - c$  plane for the HDE model (*Right*). Note that here the NADE model is regarded as a two-parameter model. The star denotes the best fit.

TABLE I: The fit values for the NADE and HDE models. Note that here the NADE model is regarded as a two-parameter model.

Model	$\Omega_{m0}$	$n/c$	$\chi^2_{min}$
NADE	$0.270^{+0.021}_{-0.020} (1\sigma)_{-0.033}^{+0.036} (2\sigma)$	$206.762^{+131.212}_{-69.060} (1\sigma)_{-71.610}^{+131.212} (2\sigma)$	542.915
HDE	$0.276^{+0.022}_{-0.020} (1\sigma)_{-0.033}^{+0.036} (2\sigma)$	$0.748^{+0.095}_{-0.085} (1\sigma)_{-0.134}^{+0.164} (2\sigma)$	543.056

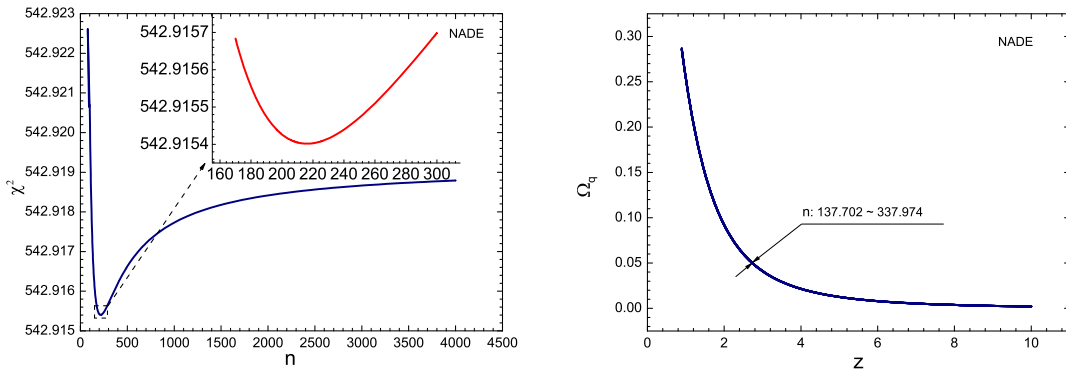


FIG. 3: (color online) Left panel: the plot of  $\chi^2$  versus  $n$  for the two-parameter NADE model with  $\Omega_{m0} = 0.270$ . Right panel: the plot of  $\Omega_q$  versus  $z$  for the two-parameter NADE model with  $n$  varying from 137.702 to 337.974.

model. The equation of motion for the HDE fractional density  $\Omega_\Lambda$  is given by [30]

$$\Omega'_\Lambda = \Omega_\Lambda (1 - \Omega_\Lambda) \left( 1 + \frac{2}{c} \sqrt{\Omega_\Lambda} \right), \quad (34)$$

where  $c$  is a numerical parameter similar to  $n$  in the NADE model. Using  $\frac{d}{dx} = -(1+z)\frac{d}{dz}$ , we get

$$\frac{d\Omega_\Lambda}{dz} = -\frac{\Omega_\Lambda}{1+z} \left( 1 + \frac{2}{c} \sqrt{\Omega_\Lambda} \right). \quad (35)$$

In Figure 2 (*Right*), we plot contours of the  $1\sigma$  and  $2\sigma$  confidence levels in the  $\Omega_{m0}-c$  plane for the HDE model. The fit values for the model parameters are also presented in Table I.

Comparing with the HDE model, we find that the NADE model has a lower  $\chi_{min}^2$ . Notwithstanding, it is obviously seen from Figure 3 (*Left*) that the data does not effectively constrain the parameter  $n$ , i.e., a very large range of values of  $n$  are allowed by the data. Figure 3 (*Left*) shows the plot of  $\chi^2$  versus  $n$  with fixed  $\Omega_{m0}$  (which is fixed to the best fit value of 0.270). One should notice that  $\chi^2$  tends to be a constant as  $n$  becomes large and the value of the constant  $\chi^2$  is just slightly larger than  $\chi_{min}^2$ . It is, therefore, not surprising that  $n$  can range in value from 137.702 to 337.974 at the  $1\sigma$  level. Now, let us discuss the cosmological consequence of such a strong degeneracy of  $n$ . For this purpose, we plot the evolution of  $\Omega_q(z)$  with  $n$  varying from 137.702 (the lower limit value at  $1\sigma$ ) to 337.974 (the upper limit value at  $1\sigma$ ) in Figure 3 (*Right*). We see that the curves with different  $n$  are almost totally degenerate in a narrow region. This indicates that the cosmological evolution tends to be the same when  $n$  takes large values in this model. In fact, we can also infer this from (7). We notice that the term  $\frac{2(1+z)}{n} \sqrt{\Omega_q}$  is negligible when  $n$  is large enough. Thus, (7) reduces to

$$\frac{d\Omega_q}{dz} = -\frac{3\Omega_q}{1+z} (1 - \Omega_q). \quad (36)$$

Solving this equation we obtain  $\rho_q = \text{constant}$ . Therefore, from the above analysis, we find that when the NADE model is regarded as a two-parameter model, the dark energy is more likely to behave as a cosmological constant. So, in the rest of this paper, we confine our discussions to the single-parameter NADE model.

Next, we discuss the cases of the INADE model. Different cases of this model are denoted as INADE1, INADE2, INADE3 and INADE4, respectively. Table II summarizes the fitting results for the four cases of the INADE model. For comparison, we also list the results of the NADE model. In this table we show the best fit,  $1\sigma$  and  $2\sigma$  values of the parameters and the  $\chi_{min}^2$  values of the models. The best fit gives values of  $h = 0.692, 0.690, 0.691$  and  $0.688$  and  $\Omega_{m0} = 0.240, 0.236, 0.237$  and  $0.239$  for the four interacting cases. One can see from Table II that the INADE1, INADE2 and INADE3 models have a

similar  $\chi_{min}^2$ , and the INADE4 model gives a larger  $\chi_{min}^2$  than the other three, but all are lower than the NADE model. In addition, a distinctive feature in the INADE4 model is that the fit values of parameter  $b$  are all negative in the  $2\sigma$  range. As discussed in the previous section, a negative  $b$  would lead to a negative  $\rho_m$  in the future. So, in this sense, we have shown that the INADE4 model is not a reasonable model according to the observational data analysis. For the  $1\sigma$  and  $2\sigma$  contours in the  $n-b$  plane for the four INADE models, we refer the reader to Figure 5. We will now discuss the high- $z$  cosmic age problem caused by the old quasar APM 08279+5255 at redshift  $z = 3.91$ .

#### IV. AGE PROBLEM: CHALLENGE AND WAY OUT

The age of the universe at redshift  $z$  is given by

$$t(z) = \int_z^\infty \frac{dz'}{(1+z')H(z')}. \quad (37)$$

It is convenient to introduce a dimensionless cosmic age

$$T_{cos}(z) \equiv H_0 t(z) = \int_z^\infty \frac{dz'}{(1+z')E(z')}, \quad (38)$$

where  $E(z) \equiv H(z)/H_0$ . At any given redshift, the age of the universe should not be less than the age of any object in the universe, namely,  $T_{cos}(z) \geq T_{obj}(z) \equiv H_0 t_{obj}(z)$ , where  $t_{obj}(z)$  is the age of an OHRO at redshift  $z$ . For convenience, we define a dimensionless quantity, the ratio of the cosmic and OHRO ages,

$$\tau(z) \equiv \frac{T_{cos}(z)}{T_{obj}(z)} = H_0^{-1} t_{obj}^{-1}(z) \int_z^\infty \frac{dz'}{(1+z')E(z')}. \quad (39)$$

Thus, the condition  $\tau(z) \geq 1$  is equivalent to  $T_{cos}(z) \geq T_{obj}(z)$ .

First, we will test the NADE model with the ages of the OHROs. We will use three OHROs: the old galaxy LBDS 53W091 at redshift  $z = 1.55$ , the old galaxy LBDS 53W069 at  $z = 1.43$  and the old quasar APM 08279+5255 at  $z = 3.91$ . The ages of the OHROs at  $z = 1.55$  and  $z = 1.43$  are 3.5 Gyr and 4.0 Gyr, respectively. For the age of the OHRO at  $z = 3.91$ , following [25], we use the lower bound estimate of  $t_{obj}(3.91) = 2.0$  Gyr. We calculate the age of the universe at different redshifts using the best fit results of the NADE model,  $n = 2.886$  and  $h = 0.685$ , and then we obtain the values of  $\tau$ :  $\tau(1.55) = 1.215$ ,  $\tau(1.43) = 1.136$ , and  $\tau(3.91) = 0.833$ , also shown in Table III. So, the NADE model can easily accommodate the OHROs at  $z = 1.55$  and  $1.43$ , but cannot accommodate the old quasar at  $z = 3.91$ . Of course, the above result is only for the best fit. We will now see if the old quasar can be accommodated within the  $2\sigma$  range. We show the result in Figure 4. In this figure, the blue line represents  $\tau(3.91)$

TABLE II: The fit values for the NADE and INADE models.

Model	$n$	$b$	$\chi^2_{min}$
NADE	$2.886^{+0.084}_{-0.082} (1\sigma)^{+0.169}_{-0.163} (2\sigma)$	N/A	571.338
INADE1	$3.199^{+0.194}_{-0.181} (1\sigma)^{+0.324}_{-0.290} (2\sigma)$	$0.029^{+0.008}_{-0.009} (1\sigma)^{+0.014}_{-0.015} (2\sigma)$	552.674
INADE2	$3.245^{+0.218}_{-0.202} (1\sigma)^{+0.364}_{-0.322} (2\sigma)$	$0.016^{+0.006}_{-0.006} (1\sigma)^{+0.010}_{-0.010} (2\sigma)$	556.492
INADE3	$3.236^{+0.207}_{-0.193} (1\sigma)^{+0.344}_{-0.307} (2\sigma)$	$0.010^{+0.003}_{-0.004} (1\sigma)^{+0.006}_{-0.006} (2\sigma)$	555.015
INADE4	$3.208^{+0.239}_{-0.214} (1\sigma)^{+0.406}_{-0.339} (2\sigma)$	$-0.027^{+0.013}_{-0.015} (1\sigma)^{+0.022}_{-0.025} (2\sigma)$	561.634

with  $n$  running over the  $2\sigma$  range; for simplicity, we fix  $h$  to the best fit value in the calculation. It is clear that the NADE model does not accommodate the old quasar APM 08279+5255, therefore, this age problem raises a serious challenge to the NADE model.

To overcome this difficulty, we seek help from the possible interaction between dark energy and dark matter. Thus, we next explore whether the old quasar APM 08279+5255 can be accommodated in the INADE model. Based on the above results of observational constraints, we can easily accomplish this task. Using the best-fit values, we obtain the values of  $\tau(z)$  for the four INADE models, listed in Table III. One can see that the  $\tau(z)$  values indeed increase when the interaction is included in the model. Notwithstanding, for the old quasar at  $z = 3.91$ , the values of  $\tau(3.91)$  only increase from 0.83 to about 0.92, still not exceeding the value 1. So, if only considering the best fit, the INADE models cannot solve the age crisis. Of course, it is evident that the age problem has been greatly alleviated via the interaction between dark energy and dark matter. As the next step, we will scan the full parameter space to explore whether there exists an area able to realize  $\tau(3.91) > 1$ . We show the result in Figure 5. The red line indicates where  $\tau(3.91) = 1$ , using the best fit value for  $h$ , and thus the region to the right denotes  $\tau(3.91) > 1$ , as indicated by the arrows. From this figure, one can clearly see that the red line passes through the  $2\sigma$  region of the  $n - b$  parameter space of the first three INADE models. For the fourth case, INADE4, the red line only intersects the edge of the  $2\sigma$  region. This result again shows that the form of interaction  $Q = 3bH(\rho_q - \rho_m)$  is not reasonable, since it not only has a negative  $b$ , but also fails to provide a solution to the high- $z$  cosmic age problem.

The above analysis indicates that the old quasar APM 08279+5255 can be successfully accommodated by the INADE model (at least for three cases) at the  $2\sigma$  level. There indeed exists an area within the  $2\sigma$  scope where  $\tau(3.91) > 1$  is realized, and thus, it successfully solves the age crisis of the NADE model. To be modest, we do not assert that the cosmic age crisis has been completely solved by the INADE model. After all, only a small area and not the full region of the  $2\sigma$  scope resides to the right of the  $\tau(3.91) = 1$  red line. However, it should be noted that the age problem has been significantly alleviated by the INADE model under the current observational

constraints.

Finally, we feel that it would be better if some additional comments on the age problem are given. The age problem is seen in the apparent old age of a single quasar, APM 08279+5255, whose high Fe/O ratio derived from X-ray observations has been used to argue for an age of at least 2 Gyr. At the quasar's redshift of 3.91, the standard  $\Lambda$ CDM model is only 1.6 Gyr old and thus apparently younger than the quasar itself. However, the age estimate of the quasar rests on the assumption that star formation and evolution proceeds in a way similar to that observed in the late universe. It is not even the absolute amount of Fe that serves as an argument, but the relative Fe/O abundance. Sub-millimeter observations show, however, that star formation seems to proceed in an atypical way in APM 08279+5255 [51]. This sheds doubt on the age estimate itself as well as on its reliability. Nevertheless, until a more accurate measurement of the age of the quasar is available, theorists have to seriously take the age problem into account. Likewise, a similar problem of star formation and evolution also exists for the high- $z$  SNIa, but the observational result of the cosmic acceleration is still the mainstream. So, it is believed that the discussion of the age problem in the NADE model is meaningful and significant at the current stage. Of course, we do expect that future, more accurate measurements of the age of this old quasar will naturally eliminate the age crisis in dark energy models.

## V. CONCLUSION

The agegraphic dark energy model originates from the holographic principle of quantum gravity, so it has physical significance not only in a phenomenological aspect, but also in a theoretical one. Though the NADE model has been discussed extensively, it undoubtedly deserves further investigations. In this paper, we discuss the age problem in the NADE model.

There is a lot of work addressing the age problem caused by the old quasar APM 08279+5255 at redshift  $z = 3.91$ , because this quasar has led many dark energy models into trouble, the  $\Lambda$ CDM and holographic dark energy models being no exception. We found in this paper that the NADE model is also afflicted by the age problem. So, we explore whether the inclusion of the in-

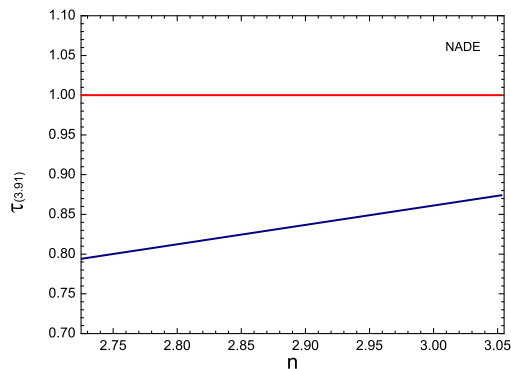


FIG. 4: (color online) The plot of  $\tau(3.91)$  versus  $n$  for the NADE model. The region avoiding the age problem is that above the  $\tau(3.91) = 1$  line (red).

TABLE III: The values of  $\tau(z)$  in the NADE, INADE1, INADE2, INADE3 and INADE4 models at best fit concerning LBDS 53W091 at  $z = 1.55$ , LBDS 53W069 at  $z = 1.43$ , and the old quasar APM 08279+5255 at  $z = 3.91$ .

Model ( $n, b, h$ )	$\tau(1.55)$	$\tau(1.43)$	$\tau(3.91)$
NADE (2.886, 0, 0.685)	1.215	1.136	0.833
INADE1 (3.199, 0.029, 0.692)	1.326	1.238	0.919
INADE2 (3.245, 0.016, 0.690)	1.318	1.230	0.923
INADE3 (3.236, 0.010, 0.691)	1.323	1.235	0.923
INADE4 (3.208, -0.027, 0.688)	1.290	1.204	0.908

teraction between dark energy and dark matter in this model can solve the age problem.

First, we used current observational data to constrain the NADE and INADE models. For the data, we use the SNIa Union2 sample, the CMB shift parameter  $R$  from 7-yr WMAP, and the BAO parameter  $A$  from the SDSS. We determined the age of the universe in the NADE model by using the fit results and found that the NADE model cannot realize  $\tau(3.91) > 1$  within the full parameter space. We also explored the cosmological consequence of regarding the NADE model as a two-parameter model. The fit results show that in such a model the dark energy is more likely to behave as a cosmological constant.

For the possible interaction between dark energy and dark matter, we considered four phenomenological cases:  $Q = 3bH\rho_q$ ,  $Q = 3bH\rho_m$ ,  $Q = 3bH(\rho_q + \rho_m)$  and  $Q = 3bH(\rho_q - \rho_m)$ . The observational data favor a positive  $b$  for the three cases, but give a negative  $b$  for the fourth case. We found that when the interaction is taken into account, the age problem caused by the quasar can be successfully solved in the first three cases of the INADE model, at the  $2\sigma$  level. The isoline  $\tau(3.91) = 1$  passes through the  $2\sigma$  region of the  $n - b$  parameter

space of the INADE model. So, there indeed exists an area within the  $2\sigma$  scope realizing  $\tau(3.91) > 1$  and thus this model successfully solves the age crisis of the NADE model. Though we cannot assert that the age crisis has been eliminated in the INADE model, since most of the parameter space is still in the troubled area and only the lower bound age of the quasar is used in the test, we are sure that the age problem has been significantly alleviated in the INADE model under the current observational constraints. Therefore, our work can be viewed as further support of the INADE model.

### Acknowledgments

We would like to thank Xiao-Dong Li for useful discussion and kind help. This work was supported by the Natural Science Foundation of China under Grant Nos. 10705041 and 10975032, as well as the National Ministry of Education of China under the innovation program for undergraduate students.

[1] Riess A G, et al. [Supernova Search Team Collaboration] Observational evidence from supernovae for an accelerating universe and a cosmological constant. *Astron*

J, 1998, 116: 1009-1038, arXiv: astro-ph/9805201; Perlmutter S, et al. [Supernova Cosmology Project Collaboration] Measurements of  $\Omega$  and  $\Lambda$  from 42 high-redshift



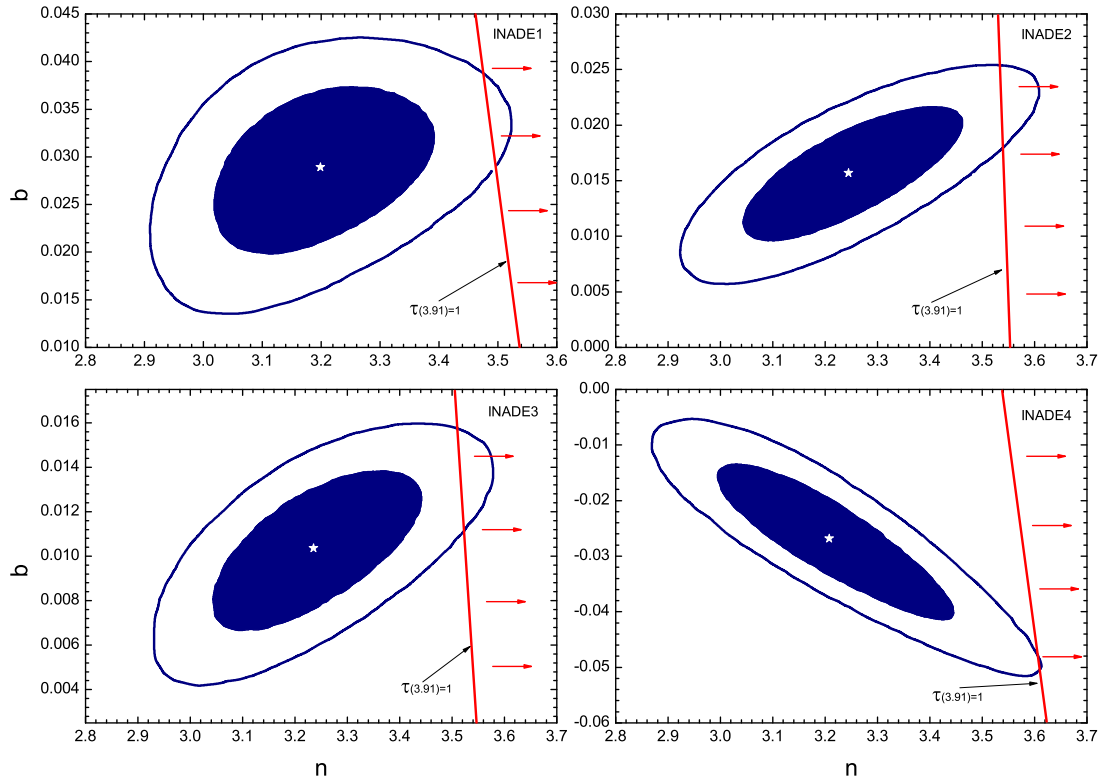


FIG. 5: (color online) The probability contours at the  $1\sigma$  and  $2\sigma$  confidence levels in the  $b - n$  plane for the four INADE models. The red line is an isoline with  $\tau(3.91) = 1$ . The allowed region avoiding the age problem is to the right of this line, as indicated by the arrows.

- supernovae. *Astrophys J*, 1999, 517: 565-586, arXiv: astro-ph/9812133.
- [2] Tegmark M, et al. [SDSS Collaboration] Cosmological parameters from SDSS and WMAP. *Phys Rev D*, 2004, 69: 103501 arXiv: astro-ph/0310723; Abazajian K, et al. [SDSS Collaboration] The second data release of the Sloan Digital Sky Survey. *Astron J*, 2004, 128: 502-512, arXiv: astro-ph/0403325; Abazajian K, et al. [SDSS Collaboration] The third data release of the Sloan Digital Sky Survey. *Astron J*, 2005, 129: 1755-1759, arXiv: astro-ph/0410239.
- [3] Spergel D N, et al. [WMAP Collaboration] First year Wilkinson Microwave Anisotropy Probe (WMAP) observations: Determination of Cosmological Parameters. *Astrophys J Suppl*, 2003, 148: 175-194, arXiv: astro-ph/0302209.
- [4] Weinberg S. The cosmological constant problem. *Rev Mod Phys*, 1989, 61: 1-23; Carroll S M. The cosmological constant. *Living Rev Rel*, 2001, 4: 1, arXiv: astro-ph/0004075.
- [5] Peebles P J E and Ratra B. Cosmology with a time variable cosmological 'constant'. *Astrophys J*, 1988, 325: L17-L20; Ratra B and Peebles P J E. Cosmological consequences of a rolling homogeneous scalar field. *Phys Rev D*, 1988, 37: 3406-3427; Wetterich C. Cosmology and the fate of dilatation symmetry. *Nucl Phys B*, 1988, 302: 668-696; Zlatev I, Wang L M and Steinhardt P J. Quintessence, cosmic coincidence, and the cosmological constant. *Phys Rev Lett*, 1999, 82: 896-899, arXiv: astro-ph/9807002; Zhang X. Reconstructing holographic quintessence. *Phys Lett B*, 2007, 648: 1-7, arXiv: astro-ph/0604484.
- [6] Armendariz-Picon C, Mukhanov V F and Steinhardt P J. A dynamical solution to the problem of a small cosmological constant and late-time cosmic acceleration. *Phys Rev Lett*, 2000, 85: 4438-4441, arXiv: astro-ph/0004134; Armendariz-Picon C, Mukhanov V F and Steinhardt P J. Essentials of  $k$ -essence. *Phys Rev D*, 2001, 63: 103510, arXiv: astro-ph/0006373.
- [7] Sen A. Tachyon matter. *J High Energy Phys*, 2002, 0207: 065, arXiv: hep-th/0203265; Padmanabhan T. Accelerated expansion of the universe driven by tachyonic matter. *Phys Rev D*, 2002, 66: 021301, arXiv: hep-th/0204150; Zhang J, Zhang X and Liu H. Holographic tachyon model. *Phys Lett B*, 2007, 651: 84-88, arXiv: 0706.1185[astro-ph].
- [8] Caldwell R R, Kamionkowski M and Weinberg N N. Phantom energy and cosmic doomsday. *Phys Rev Lett*, 2003, 91: 071301, arXiv: astro-ph/0302506; Guo Z K, Piao Y S and Zhang Y Z. Attractor behavior of phantom cosmology. *Phys Lett B*, 2004, 594: 247-251, arXiv: astro-ph/0404225; Zhang X. Can black holes be torn up by phantom dark energy in cyclic cosmology?. *Eur Phys J C*, 2009, 60: 661-667, arXiv: 0708.1408[gr-qc].

- [9] Feng B, Wang X L and Zhang X M. Dark energy constraints from the cosmic age and supernova. *Phys Lett B*, 2005, 607: 35-41, arXiv: astro-ph/0404224; Guo Z K, Piao Y S, Zhang X M and Zhang Y Z. Cosmological evolution of a quintom model of dark energy. *Phys Lett B*, 2005, 608: 177-182, arXiv: astro-ph/0410654; Zhang X. An interacting two-fluid scenario for quintom dark energy. *Commun Theor Phys*, 2005, 44: 762-768; Cai Y F, Saridakis E N, Setare M R and Xia J Q. Quintom cosmology: Theoretical implications and observations. *Phys Rept*, 2010, 493: 1-60, arXiv: 0909.2776[hep-th].
- [10] Deffayet C, Dvali G R and Gabadadze G. Accelerated universe from gravity leaking to extra dimensions. *Phys Rev D*, 2002, 65: 044023, arXiv: astro-ph/0105068; Sahni V and Shtanov Y. Braneworld models of dark energy. *J Cosmol Astropart Phys*, 2003, 0311: 014, arXiv: astro-ph/0202346; Guo W L and Zhang X. Constraints on dark matter annihilation cross section in the braneworld and quintessence scenarios. *Phys Rev D*, 2009, 79: 115023, arXiv: 0904.2451[hep-ph]; Feng C J and Zhang X. Holographic Ricci dark energy in Randall-Sundrum braneworld: Avoidance of big rip and steady state future. *Phys Lett B*, 2009, 680: 399-403, arXiv: 0904.0045[gr-qc].
- [11] Kamenshchik A Y, Moschella U and Pasquier V. An alternative to quintessence. *Phys Lett B*, 2001, 511: 265-268, arXiv: gr-qc/0103004; Bento M C, Bertolami O and Sen A A. Generalized Chaplygin gas, accelerated expansion and dark energy-matter unification. *Phys Rev D*, 2002, 66: 043507, arXiv: gr-qc/0202064; Zhang X, Wu F Q and Zhang J. New generalized Chaplygin gas as a scheme for unification of dark energy and dark matter. *J Cosmol Astropart Phys*, 2006, 0601: 003, arXiv: astro-ph/0411221.
- [12] Amendola L. Coupled quintessence. *Phys Rev D*, 2000, 62: 043511, arXiv: astro-ph/9908023; Comelli D, Pietroni M and Riotto A. Dark energy and dark matter. *Phys Lett B*, 2003, 571: 115-120, arXiv: hep-ph/0302080; Zhang X. Coupled quintessence in a power-law case and the cosmic coincidence problem. *Mod Phys Lett A*, 2005, 20: 2575, arXiv: astro-ph/0503072; Zhang X. Statefinder diagnostic for coupled quintessence. *Phys Lett B*, 2005, 611: 1-7, arXiv: astro-ph/0503075; Cai R G and Wang A. Cosmology with interaction between phantom dark energy and dark matter and the coincidence problem. *J Cosmol Astropart Phys*, 2005, 0503: 002, arXiv: hep-th/0411025; Zhang J, Liu H and Zhang X. Statefinder diagnosis for the interacting model of holographic dark energy. *Phys Lett B*, 2008, 659: 26-33, arXiv: 0705.4145[astro-ph]; He J H, Wang B and Zhang P. The imprint of the interaction between dark sectors in large scale cosmic microwave background anisotropies. *Phys Rev D*, 2009, 80: 063530, arXiv: 0906.0677[gr-qc].
- [13] Li M, Lin C and Wang Y. Some issues concerning holographic dark energy. *J Cosmol Astropart Phys*, 2008, 0805: 023, arXiv: 0801.1407[astro-ph]; Li M, Li X D, Wang S, Wang Y and Zhang X. Probing interaction and spatial curvature in the holographic dark energy model. *J Cosmol Astropart Phys*, 2009, 0912: 014, arXiv: 0910.3855[astro-ph.CO].
- [14] Sahni V and Starobinsky A A. The case for a positive cosmological  $\Lambda$ -term. *Int J Mod Phys D*, 2000, 9: 373-444, arXiv: astro-ph/9904398; Peebles P J E and Ratra B. The cosmological constant and dark energy. *Rev Mod Phys*, 2003, 75: 559-606, arXiv: astro-ph/0207347; Sahni V. Dark matter and dark energy. *Lect Notes Phys*, 2004, 653: 141-180, arXiv: astro-ph/0403324; Copeland E J, Sami M and Tsujikawa S. Dynamics of dark energy. *Int J Mod Phys D*, 2006, 15: 1753-1936, arXiv: hep-th/0603057; Frieman J, Turner M and Huterer D. Dark energy and the accelerating universe. *Ann Rev Astron Astrophys*, 2008, 46: 385-432, arXiv: 0803.0982[astro-ph]; Li M, Li X D, Wang S and Wang Y. Dark energy. arXiv: 1103.5870[astro-ph.CO].
- [15] Dunlop J, Peacock J, Spinrad H, Dey A, Jimenez R, Stern D and Windhorst R. A 3.5-Gyr-old galaxy at redshift 1.55. *Nature*, 1996, 381: 581-584; Spinrad H, Dey A, Stern D, Dunlop J, Peacock J, Jimenez R and Windhorst R. LBDS 53W091: An old red galaxy at  $z=1.552$ . *Astrophys J*, 1997, 484: 581-601, arXiv: astro-ph/9702233.
- [16] Dunlop J. Old stellar populations in distant radio galaxies. arXiv: astro-ph/9801114.
- [17] Hasinger G, Schartel N and Komossa S. Discovery of an ionized Fe-K edge in the  $z = 3.91$  broad absorption line quasar APM 08279+5255 with XMM-Newton. *Astrophys J*, 2002, 573: L77-L80, arXiv: astro-ph/0207005; Komossa S and Hasinger G. The X-ray evolving universe: (ionized) absorption and dust, from nearby Seyfert galaxies to high-redshift quasars. arXiv: astro-ph/0207321.
- [18] Alcaniz J S and Lima J A S. New limits on  $\Omega_\Lambda$  and  $\Omega_M$  from old galaxies at high redshift. *Astrophys J*, 1999, 521: L87-L90, arXiv: astro-ph/9902298; Friaca A, Alcaniz J and Lima J A S. An old quasar in a young dark energy-dominated universe?. *Mon Not Roy Astron Soc*, 2005, 362: 1295-1300, arXiv: astro-ph/0504031; Alcaniz J S, Lima J A S and Cunha J V. Cosmological implications of the APM 08279+5255, an old quasar at  $z = 3.91$ . *Mon Not Roy Astron Soc*, 2003, 340: L39-L42, arXiv: astro-ph/0301226; Yang R J and Zhang S N. The age problem in  $\Lambda$ CDM model. *Mon Not Roy Astron Soc*, 2010, 407: 1835-1841, arXiv: 0905.2683[astro-ph.CO]; Wang S, Li X D and Li M. Revisit of cosmic age problem. *Phys Rev D*, 2010, 82: 103006, arXiv: 1005.4345[astro-ph.CO].
- [19] Dantas M A, Alcaniz J S, Jain D and Dev A. Age constraints on the cosmic equation of state. *Astron Astrophys*, 2007, 467: 421, arXiv: astro-ph/0607060.
- [20] Capozziello S, Dunsby P K S, Piedipalumbo E and Rubano C. Constraining scalar-tensor quintessence by cosmic clocks. arXiv: 0706.2615[astro-ph].
- [21] Movahed M S, Baghram S and Rahvar S. Consistency of  $f(R) = \sqrt{R^2 - R_0^2}$  gravity with the cosmological observations in Palatini formalism. *Phys Rev D*, 2007, 76: 044008, arXiv: 0705.0889[astro-ph].
- [22] Movahed M S, Farhang M and Rahvar S. Recent observational constraints on the DGP modified gravity. *Int J Theor Phys*, 2009, 48: 1203-1230, arXiv: astro-ph/0701339; Movahed M S and Ghassemi S. Is thick brane model consistent with the recent observations?, *Phys Rev D*, 2007, 76: 084037, arXiv: 0705.3894[astro-ph]; Pires N, Zhu Z H and Alcaniz J S. Lookback time as a test for brane cosmology. *Phys Rev D*, 2006, 73: 123530, arXiv: astro-ph/0606689.
- [23] Rahvar S and Movahed M S. Power-law parameterized quintessence model. *Phys Rev D*, 2007, 75: 023512, arXiv: astro-ph/0604206.

- [24] Wang S and Zhang Y. Alleviation of cosmic age problem in interacting dark energy model. *Phys Lett B*, 2008, 669: 201-205, arXiv: 0809.3627[astro-ph]; Tong M L and Zhang Y. Cosmic age, Statefinder and  $Om$  diagnostics in the decaying vacuum cosmology. *Phys Rev D*, 2009, 80: 023503, arXiv: 0906.3646[gr-qc].
- [25] Wei H and Zhang S N, Age problem in the holographic dark energy model, *Phys Rev D*, 2007, 76: 063003, arXiv: 0707.2129[astro-ph]; Cui J and Zhang X. Cosmic age problem revisited in the holographic dark energy model. *Phys Lett B*, 2010, 690: 233-238, arXiv: 1005.3587[astro-ph.CO].
- [26] Zhang Y, Li H, Wu X, Wei H and Cai R G. Age constraints on the agegraphic dark energy model. arXiv: 0708.1214[astro-ph].
- [27] Witten E. The cosmological constant from the viewpoint of string theory. arXiv: hep-ph/0002297.
- [28] Hoft G. t. Dimensional reduction in quantum gravity. arXiv: gr-qc/9310026; Susskind L. The world as a hologram. *J Math Phys*, 1995, 36: 6377-6396, arXiv: hep-th/9409089; Bousso R, The holographic principle. *Rev Mod Phys*, 2002, 74: 825-874, arXiv: hep-th/0203101.
- [29] Cohen A G, Kaplan D B and Nelson A E. Effective field theory, black holes, and the cosmological constant. *Phys Rev Lett*, 1999, 82: 4971-4974, arXiv: hep-th/9803132; Hsu S D H. Entropy bounds and dark energy. *Phys Lett B*, 2004, 594: 13-16, arXiv: hep-th/0403052.
- [30] Li M. A model of holographic dark energy. *Phys Lett B*, 2004, 603: 1-5, arXiv: hep-th/0403127.
- [31] Zhang X and Wu F Q. Constraints on holographic dark energy from type Ia supernova observations. *Phys Rev D*, 2005, 72: 043524, arXiv: astro-ph/0506310; Zhang X and Wu F Q. Constraints on holographic dark energy from latest supernovae, galaxy clustering, and cosmic microwave background anisotropy observations. *Phys Rev D*, 2007, 76: 023502, arXiv: astro-ph/0701405; Huang Q G and Gong Y G. Supernova constraints on a holographic dark energy model. *J Cosmol Astropart Phys*, 2004, 0408: 006, arXiv: astro-ph/0403590; Chang Z, Wu F Q and Zhang X. Constraints on holographic dark energy from X-ray gas mass fraction of galaxy clusters. *Phys Lett B*, 2006, 633: 14-18, arXiv: astro-ph/0509531.
- [32] Huang Q G and Li M. The holographic dark energy in a non-flat universe. *J Cosmol Astropart Phys*, 2004, 0408: 013, arXiv: astro-ph/0404229; Huang Q G and Li M. Anthropic principle favors the holographic dark energy. *J Cosmol Astropart Phys*, 2005, 0503: 001, arXiv: hep-th/0410095; Zhang X. Statefinder diagnostic for holographic dark energy model. *Int J Mod Phys D*, 2005, 14: 1597-1606, arXiv: astro-ph/0504586; Zhang X. Dynamical vacuum energy, holographic quintom, and the reconstruction of scalar-field dark energy. *Phys Rev D*, 2006, 74: 103505, arXiv: astro-ph/0609699; Ma Y Z and Zhang X. Theoretical limits of holographic quintessence. *Phys Lett B*, 2008, 661: 239-245, arXiv: 0709.1517[astro-ph]; Wu X and Zhu Z H. Reconstructing  $f(R)$  theory according to holographic dark energy. *Phys Lett B*, 2008, 660: 293-298, arXiv: 0712.3603[astro-ph]; Zhang J, Zhang X and Liu H. Holographic dark energy in a cyclic universe. *Eur Phys J C*, 2007, 52: 693-699, arXiv: 0708.3121[hep-th]; Gong Y G. Extended holographic dark energy. *Phys Rev D*, 2004, 70: 064029, arXiv: hep-th/0404030; Wang B, Abdalla E and Su R K. Constraints on the dark energy from holography. *Phys Lett B*, 2005, 611: 21-26, arXiv: hep-th/0404057; Wu X, Cai R G and Zhu Z H. Dynamics of holographic vacuum energy in the DGP model. *Phys Rev D*, 2008, 77: 043502, arXiv: 0712.3604 [astro-ph]; Li M, Li X D, Lin C and Wang Y. Holographic Gas as Dark Energy. *Commun Theor Phys*, 2009, 51: 181-186, arXiv: 0811.3332[hep-th]; Wang B, Gong Y G and Abdalla E. Transition of the dark energy equation of state in an interacting holographic dark energy model. *Phys Lett B*, 2005, 624: 141-146, arXiv: hep-th/0506069; Wang B, Lin C Y and Abdalla E. Constraints on the interacting holographic dark energy model. *Phys Lett B*, 2006, 637: 357-361, arXiv: hep-th/0509107; Zhang X. Heal the world: Avoiding the cosmic doomsday in the holographic dark energy model. *Phys Lett B*, 2010, 683: 81-87, arXiv: 0909.4940[gr-qc]; Liu D J, Wang H and Yang B. Modified holographic dark energy in DGP brane world. *Phys Lett B*, 2010, 694: 6-9, arXiv: 1009.3776[astro-ph.CO].
- [33] Cai R G. A dark energy model characterized by the age of the universe. *Phys Lett B*, 2007, 657: 228-231, arXiv: 0707.4049[hep-th].
- [34] Károlyházy F. Gravitation and quantum mechanics of macroscopic objects. *Nuovo Cim A*, 1966, 42: 390-402; Károlyházy F, Frenkel A and Lukács B. Physics as Natural Philosophy. In: Simonyi A, Feschbach H, eds. Cambridge, MA: MIT Press, 1982; Károlyházy F, Frenkel A and Lukács B, Quantum Concepts in Space and Time. In: Penrose R, Isham C J, eds. Oxford: Clarendon Press, 1986.
- [35] Wei H and Cai R G. A new model of agegraphic dark energy. *Phys Lett B*, 2008, 660: 113-117, arXiv: 0708.0884[astro-ph].
- [36] Wei H and Cai R G. Cosmological constraints on new agegraphic dark energy. *Phys Lett B*, 2008, 663: 1-6, arXiv: 0708.1894[astro-ph]; Li M, Li X D, Wang S and Zhang X. Holographic dark energy models: A comparison from the latest observational data. *J Cosmol Astropart Phys*, 2009, 0906: 036, arXiv: 0904.0928[astro-ph.CO]; Li M, Li X D and Zhang X. Comparison of dark energy models: A perspective from the latest observational data. *Sci China Phys Mech Astron*, 2010, 53: 1631-1645, arXiv: 0912.3988[astro-ph.CO]; Wei H. Observational constraints on cosmological models with the updated long gamma-ray bursts. *J Cosmol Astropart Phys*, 2010, 1008: 020, arXiv: 1004.4951[astro-ph.CO]; Zhang J, Zhang L and Zhang X. Sandage-Loeb test for the new agegraphic and Ricci dark energy models. *Phys Lett B*, 2010, 691: 11-17, arXiv: 1006.1738[astro-ph.CO].
- [37] Neupane I P. Remarks on dynamical dark energy measured by the conformal age of the universe. *Phys Rev D*, 2007, 76: 123006, arXiv: 0709.3096[hep-th]; Zhang J, Zhang X and Liu H. Agegraphic dark energy as a quintessence. *Eur Phys J C*, 2008, 54: 303-309, arXiv: 0801.2809[astro-ph]; Kim Y W, Lee H W, Myung Y S and Park M I. New agegraphic dark energy model with generalized uncertainty principle. *Mod Phys Lett A*, 2008, 23: 3049-3055, arXiv: 0803.0574 [gr-qc]; Wu J P, Ma D Z and Ling Y. Quintessence reconstruction of the new agegraphic dark energy model. *Phys Lett B*, 2008, 663: 152-159, arXiv: 0805.0546 [hep-th]; Cui J, Zhang L, Zhang J and Zhang X. New agegraphic dark energy as a rolling tachyon. *Chin Phys B*, 2010, 19: 019802, arXiv: 0902.0716[astro-ph.CO]; Liu X L and

- Zhang X. New agegraphic dark energy in Brans-Dicke theory. *Commun Theor Phys*, 2009, 52: 761-768, arXiv: 0909.4911[astro-ph.CO]; Liu X L, Zhang J and Zhang X. Theoretical limits on agegraphic quintessence from weak gravity conjecture. *Phys Lett B*, 2010, 689: 139-144, arXiv: 1005.2466 [gr-qc]; Setare M R. New agegraphic dark energy in  $f(R)$  gravity. *Astrophys Space Sci*, 2010, 326: 27-31, arXiv: 0908.0196[gr-qc]; Sheykhi A and Setare M R. Interacting new agegraphic viscous dark energy with varying  $G$ . *Int J Theor Phys*, 2010, 49: 2777-2785, arXiv: 1003.1109[physics.gen-ph]; Jamil M and Saridakis E N. New agegraphic dark energy in Horava-Lifshitz cosmology. *J Cosmol Astropart Phys*, 2010, 1007: 028, arXiv:1003.5637 [physics.gen-ph]; Karami K, Sheykhi A, Jamil M, Azarmi Z and Soltanzadeh M M. Interacting entropy-corrected new agegraphic dark energy in Brans-Dicke cosmology. *Gen Rel Grav*, 2011, 43: 27-39, arXiv: 1004.3607[hep-th]; Malekjani M and Khodam-Mohammadi A. Interacting entropy-corrected agegraphic Chaplygin gas model of dark energy. arXiv: 1004.1017[gr-qc].
- [38] Pavon D and Wang B. Le Chatelier-Braun principle in cosmological physics. *Gen Rel Grav*, 2009, 41: 1-5, arXiv: 0712.0565[gr-qc].
- [39] Pereira S H and Jesus J F. Can dark matter decay in dark energy?. *Phys Rev D*, 2009, 79: 043517, arXiv: 0811.0099[astro-ph].
- [40] Costa F E M, Barboza E M and Alcaniz J S. Cosmology with interaction in the dark sector. *Phys Rev D*, 2009, 79: 127302, [arXiv:0905.0672 [astro-ph.CO]].
- [41] Cai R G and Su Q. On the dark sector interactions. *Phys Rev D*, 2010, 81: 103514, arXiv: 0912.1943[astro-ph.CO].
- [42] Sun C Y. Interaction between dark energy and dark matter crosses non-interacting line. arXiv: 1009.1214 [gr-qc].
- [43] Zhang L, Cui J, Zhang J and Zhang X. Interacting model of new agegraphic dark energy: Cosmological evolution and statefinder diagnostic. *Int J Mod Phys D*, 2010, 19: 21-35, arXiv: 0911.2838[astro-ph.CO].
- [44] Amanullah R, et al. Spectra and light curves of six type Ia supernovae at  $0.511 < z < 1.12$  and the union2 compilation. *Astrophys J*, 2010, 716: 712-738, arXiv: 1004.1711[astro-ph.CO].
- [45] Nesseris S and Perivolaropoulos L. Comparison of the Legacy and Gold SnIa dataset constraints on dark energy models. *Phys Rev D*, 2005, 72: 123519, arXiv: astro-ph/0511040; Perivolaropoulos L. Constraints on linear-negative potentials in quintessence and phantom models from recent supernova data. *Phys Rev D*, 2005, 71: 063503, arXiv: astro-ph/0412308; Nesseris S and Perivolaropoulos L. Tension and systematics in the Gold06 SnIa dataset. *J Cosmol Astropart Phys*, 2007, 0702: 025, arXiv: astro-ph/0612653.
- [46] Wang Y and Mukherjee P. Robust dark energy constraints from supernovae, galaxy clustering, and three-year Wilkinson Microwave Anisotropy Probe observations. *Astrophys J*, 2006, 650: 1-6, arXiv: astro-ph/0604051.
- [47] Bond J R, Efstathiou G and Tegmark M. Forecasting cosmic parameter errors from microwave background anisotropy experiments. *Mon Not Roy Astron Soc*, 1997, 291: L33-L41, arXiv: astro-ph/9702100.
- [48] Komatsu E, et al. Seven-year Wilkinson Microwave Anisotropy Probe (WMAP) observations: Cosmological interpretation. *Astrophys J Suppl*, 2011, 192: 18, arXiv: 1001.4538[astro-ph.CO].
- [49] Tegmark M, et al. [SDSS Collaboration] The 3D power spectrum of galaxies from the SDSS. *Astrophys J*, 2004, 606: 702-740, arXiv: astro-ph/0310725; Seljak U, et al. [SDSS Collaboration] Cosmological parameter analysis including SDSS Ly-alpha forest and galaxy bias: Constraints on the primordial spectrum of fluctuations, neutrino mass, and dark energy. *Phys Rev D*, 2005, 71: 103515, arXiv: astro-ph/0407372; Tegmark M, et al. [SDSS Collaboration] Cosmological constraints from the SDSS luminous red galaxies. *Phys Rev D*, 2006, 74: 123507, arXiv: astro-ph/0608632.
- [50] Eisenstein D J, et al. [SDSS Collaboration] Detection of the baryon acoustic peak in the large-scale correlation function of SDSS luminous red galaxies. *Astrophys J*, 2005, 633: 560-574, arXiv: astro-ph/0501171.
- [51] Riechers D A, Walter F, Carilli C L, Cox P, Weiss A, Bertoldi F and Menten K M. Dense molecular gas excitation at high redshift: Detection of HCO+(J=4-3) emission in the cloverleaf quasar. *Astrophys J*, 2011, 726: 50, arXiv: 1011.0991[astro-ph.CO].